Journal of Pathology
J Pathol September 2022; **258:** 12–25
Published online 6 June 2022 in Wiley Online Library
(wileyonlinelibrary.com) DOI: 10.1002/path.5924

ORIGINAL ARTICLE

CXCR4 mediates leukemic cell migration and survival in the testicular microenvironment

Tessa Skroblyn[1,2], Jara J Joedicke[3], Madlen Pfau[2], Kerstin Krüger[1], Jean-Pierre Bourquin[4], Shai Izraeli[5,6], Cornelia Eckert[2,7†*] and Uta E Höpken[1†*]

[1] *Department of Microenvironmental Regulation in Autoimmunity and Cancer, Max-Delbrück-Center for Molecular Medicine, MDC, Berlin, Germany*
[2] *Department of Pediatric Oncology, Charité-University Medicine, Campus Virchow Klinikum, Berlin, Germany*
[3] *Department of Translational Tumorimmunology, Max-Delbrück-Center for Molecular Medicine, MDC, Berlin, Germany*
[4] *Department of Pediatric Oncology, University Children's Hospital, Zurich, Switzerland*
[5] *Schneider Children's Medical Center of Israel, Petach Tiqva, Israel*
[6] *Tel Aviv University, Tel Aviv, Israel*
[7] *German Cancer Consortium, and German Cancer Research Center, Heidelberg, Germany*

**Correspondence to: U E Höpken, Max-Delbrück-Center for Molecular Medicine, MDC, Robert-Rössle-Street 10, 13125 Berlin, Germany. E-mail: uhoepken@mdc-berlin.de; C Eckert, Department of Pediatric Oncology, Charité-University Medicine, Campus Virchow Klinikum, 13353 Berlin, Germany. E-mail: cornelia.eckert@charite.de*

†Equal contributions.

Abstract

The testis is the second most frequent extramedullary site of relapse in pediatric acute lymphoblastic leukemia (ALL). The mechanism for B-cell (B) ALL cell migration towards and survival within the testis remains elusive. Here, we identified CXCL12–CXCR4 as the leading signaling axis for B-ALL cell migration and survival in the testicular leukemic niche. We combined analysis of primary human ALL with a novel patient-derived xenograft (PDX)-ALL mouse model with testicular involvement. Prerequisites for leukemic cell infiltration in the testis were prepubertal age of the recipient mice, high surface expression of CXCR4 on PDX-ALL cells, and CXCL12 secretion from the testicular stroma. Analysis of primary pediatric patient samples revealed that CXCR4 was the only chemokine receptor being robustly expressed on B-ALL cells both at the time of diagnosis and relapse. In affected patient testes, leukemic cells localized within the interstitial space in close proximity to testicular macrophages. Mouse macrophages isolated from affected testes, in the PDX model, revealed a macrophage polarization towards a M2-like phenotype in the presence of ALL cells. Therapeutically, blockade of CXCR4-mediated functions using an anti-CXCR4 antibody treatment completely abolished testicular infiltration of PDX-ALL cells and strongly impaired the overall development of leukemia. Collectively, we identified a prepubertal condition together with high CXCR4 expression as factors affecting the leukemia permissive testicular microenvironment. We propose CXCR4 as a promising target for therapeutic prevention of testicular relapses in childhood B-ALL.

Keywords: B cell acute lymphoblastic leukemia; testis relapse; chemokine receptor CXCR4; tumor microenvironment; macrophages

Received 17 October 2021; Revised 30 March 2022; Accepted 3 May 2022

No conflicts of interest were declared.

Introduction

Acute lymphoblastic leukemia (ALL) is the most common type of cancer in children. Although the majority of patients achieve long-term remission due to modern treatment protocols, relapsed ALL has poor prognosis and is the leading cause of death in childhood cancer [1,2]. Relapses usually develop in the bone marrow (BM) (medullary), but nonhematopoietic extramedullary relapses occur in about 40% of patients, most frequently in the central nervous system (CNS) (60%) and the testis (30%) [3]. Testicular relapses usually occur late (>6 months after completion of frontline treatment) [3,4], and boys belonging to the most frequent pediatric genetic subtype (*ETV6–RUNX1* fusion gene-positive) have a higher risk of testicular relapses [5]. In adult ALL, only about 1% of patients have a testicular relapse [6]. Event-free survival ranges between 40–80%, depending on the timing of relapse and involvement of the contralateral testis and the BM [4]. Surgical removal or local irradiation are the only treatment options for testicular relapses to achieve long-term event-free survival, but both impact the fertility of the patients and thereby the long-term quality of life [7]. The molecular

mechanisms regulating leukemic cell migration, growth, and survival in the testis have not been sufficiently assessed.

The presumed benign counterparts of B-ALL cells are precursor B cells that reside in the BM. Their maturation is strongly dependent on the stromal microenvironment in which CXCL12-secreting stroma becomes in contact with CXCR4-expressing precursor B cells [8]. Therefore, the CXCL12–CXCR4 signaling axis is viewed as a key niche-associated pathway that is shared across various hematological malignancies such as ALL, acute myeloid leukemia (AML), and chronic lymphocytic leukemia (CLL) [9,10]. In pediatric ALL, increased CXCR4 expression on leukemia cells is associated with liver and spleen involvement [11]. Beyond its function as a migration regulator, the CXCL12–CXCR4 axis provides paracrine growth and survival signals and proangiogenesis effects with the potential to sustain the malignant process [12].

It is not known at what disease stage migration of leukemic cells to the testis occurs, whether it is before, at initial diagnosis, or during treatment. In the testis, the CXCL12–CXCR4 axis is physiologically important *in utero* for migration of primordial germ cells and after birth to maintain the spermatogonial niche. CXCL12 is expressed predominantly by Sertoli cells surrounding the seminiferous tubuli [13–15]. The testis is an immune-privileged site and the immunosuppressive conditions might contribute to survival of leukemia cells [16]. Testis-resident macrophages are the major testicular leukocyte type and contribute to the immunosuppressive microenvironment beside their role in testis development [17–19].

To dissect the cellular requirements and molecular pathways contributing to testicular leukemic cell dissemination and survival, we: (i) analyzed chemokine receptor expression profiles of pediatric B-ALL samples from patients with different relapse sites, (ii) studied crosstalk of leukemia cell-stroma in cocultures, and (iii) established a B-ALL xenograft model with testicular involvement. The CXCR4–CXCL12 axis was identified as the driving force of B-ALL cell migration to the testicular niche, and we identified different testicular stroma cell subpopulations as a source for CXCL12. Importantly, we identified a prepubertal condition as a prerequisite for testicular infiltration of leukemic cells. Within the testicular microenvironment of tumor-challenged mice, macrophages developed a protumorigenic M2-like phenotype. Blocking the CXCL12–CXCR4 signaling axis completely abrogated testicular leukemic cell dissemination in the PDX-ALLs.

Materials and methods

Primary pediatric B-ALL patient samples and B-ALL patient-derived xenografts (PDX)

The study was conducted according to the Declaration of Helsinki and in accordance with local ethical guidelines; written informed consent of all patients was obtained. Use of primary tumor samples was approved by the Ethics Committee *Ethikausschuss* 2 of Charité-Universitätsmedizin Berlin (#EA2/056/17). B-ALL relapse and subtypes were diagnosed by expert Charité-Universitätsmedizin Berlin hematologists and pathologists.

Mononuclear cells isolated from 54 BM samples at initial and/or relapse diagnosis from 29 pediatric B-ALL patients were selected according to their relapse sites with or without involvement of the testis or the CNS. Representative paraffin-embedded testis sections were selected for immunohistochemical staining ($n = 7$). Patient-derived BM mesenchymal stem cells (BM-MSCs, $n = 11$) and testis MSC-like cells/testicular stroma ($n = 9$) isolated and characterized as described [20] were used. Cocultures were performed using mononuclear cells isolated from BM collected at relapse diagnosis ($n = 13$).

The mononuclear cells from two patients with a relapse (PDX-ALL #1064 and #1476) were used, following a second passage of NOD scid gamma (NSG) mice engraftment, for the leukemia xenotransplantation model. Both patients had an early relapse (12 months after initial diagnosis) of a B-ALL, showed morphological nonresponse to relapse treatment, and their leukemias were negative for frequent fusion genes or aneuploidies in pediatric ALL (supplementary material, Table S1).

Mice

All animal studies were performed according to institutional and Berlin State guidelines (G0104/16; G0331/19; G0279/19; G0088/20). NSG (NOD.Cg-Prkdcscid Il2rg tm1 Wjl/SzJ; CD45.1) and C57BL/6N mice were bred at the animal facility of the Max-Delbrück-Center in a specific-pathogen-free environment (temperature: 22 ± 2 °C; humidity: $55 \pm 10\%$; 12 h light / 12 h dark cycle).

Leukemia xenotransplantation model

B-ALL xenografts #1064 and #1476 expressing firefly luciferase and enhanced green fluorescent protein (eGFP) were generated as described [21]. Cells were injected intravenously (i.v.) into NSG mice. Tumor growth was detected using luciferin intraperitoneal (i.p.) application and IVIS Spectrum imaging (Perkin Elmer, Waltham, MA, USA). Living Image Version 4.5 software (Perkin Elmer) was used to analyze the bioluminescence average radiance as photons/s per cm^2 per steradian. To block the CXCL12–CXCR4 axis, B-ALL transplanted mice were treated i.p. twice weekly from day 4 after transplantation with either antihuman CXCR4 or anti-IgG2a antibody (Ab) (50 µg/mouse on days 4, 7, and 11; 100 µg/mouse on days 14, 18, and 21). Body weight of mice varied between 13–15 g at the beginning of the treatment and between 20–23 g at the last treatment.

Human cell lines and primary cells from healthy tissue

The B cell precursor leukemia cell lines Nalm6 and REH were obtained from Dr. Stephan Mathas (MDC, Berlin, Germany). The authenticity of cell lines was confirmed by a multiplex cell line authentication test (Multiplexion, Heidelberg, Germany).

In vitro coculture assays

Patient-derived stroma-tumor cell cocultures were performed with primary human relapse ALL samples in a ratio 1:10 in RPMI 1640/1% FCS/1% penicillin and streptomycin stock solution for 48 h.

Mouse cell lines

The cell lines M210B4, TM4, and EL4 were obtained from the American Type Culture Collection (ATCC, Manassas, VA, USA).

Flow cytometry analysis

Blocking and specific staining were performed as described in Supplementary materials and methods.

Statistical analysis

Results are expressed as arithmetic means ± SEM unless otherwise stated. Values of $p < 0.05$ were considered statistically significant, as determined using a two-tailed unpaired Student's *t*-test, unpaired multiple *t* test, or the Mann–Whitney *U* test, as appropriate. The statistic features of GraphPad Prism (San Diego, CA, USA) data analysis software suites were used.

Please see Supplementary materials and methods for details of reverse transcription (RT)-qPCR (with primers listed in supplementary material, Table S2), Generation of human stroma cultures from BM and testis were performed with flow cytometry analysis and cell sorting, transduction of PDX-ALL cells with Luciferase-GFP, *in vivo* IVIS imaging, chemotaxis assays, cytokine secretion assay, and immunohistology.

Results

The chemokine receptor CXCR4 is uniformly expressed on pediatric patient ALL samples at initial diagnosis and relapse

The mechanism of ALL cell homing and survival within the testicular relapse site is still unclear. Because chemokine receptors regulate migration of immune cells and their malignant counterparts [22,23], we determined their surface expression on primary BM-derived pediatric patient samples subdivided according to the relapse sites into three major groups: isolated BM relapse, combined CNS relapse, and combined testicular relapse. CXCR4 was always substantially expressed irrespective of the relapsed site (Figure 1A,B, and supplementary material, Table S3). CCR7 and CXCR3 were moderately expressed in a few samples of the isolated BM or combined CNS relapse groups; other chemokine receptors were not detectable (supplementary material, Table S3). High surface expression of CXCR4 was also confirmed on B-ALL-derived tumor cell lines representing different immune phenotypes and genetics such as REH, Nalm6, and SEM (Figure 1C).

The interleukin7 receptor (IL7R) is described as widely expressed in B-ALL, and high expression often correlates with CNS involvement and relapse [24]. The synergistic effects of IL7R with CXCR4 have been shown to drive transformation and development of ALL subtypes. We detected IL7R expression on pediatric B-ALL already at the time of initial and at relapse diagnosis (Figure 1D). Notably, B-ALL samples from patients with a combined BM/testis relapse showed increased IL7R expression compared to BM relapse only (Figure 1E).

Testicular stroma cells and BM-derived MSCs support ALL cell migration and survival

CXCR4-expressing Nalm6 cells exhibited strong migration towards the respective chemokine ligand CXCL12 in a migration assay (Figure 2A). When CXCR4 was stably knocked out (supplementary material, Figure S1A,B) Nalm6 cell migration was profoundly impaired (Figure 2A). BM-derived mesenchymal stem cells (MSCs) secrete CXCL12 and mediate migration as well as short- and long-term maintenance of ALL cells *in vitro* [25,26]. Immunostaining of leukemia-cell affected and nonaffected testis revealed CXCL12 protein expression of Sertoli cells and other yet unknown interstitial cells (Figure 2B). Additionally, CXCL12 protein expression was detected in stromal cells of a testis with massive leukemia involvement (supplementary material, Figure S2).

To test whether testicular stroma may also support recruitment and survival of ALL cells, we cultured 15 ALL patient-derived testicular and BM $CD19^{-}CD45^{-}$ stroma cell samples for 1 week and compared the expression of surface markers characteristic of MSCs. Expression levels, in particular of CD29, CD90, and CD146, were found to be higher on BM-derived compared to testis-derived stroma cells (Figure 2C). Overall, BM and testis-derived stroma cells exhibited MSC-like characteristics and were further used for cocultures with Nalm6 or primary ALL cells. First, we demonstrated that CXCL12 is secreted into the supernatant when Nalm6 cells were cocultured for 48 h with either BM-MSCs or with testis-derived stromal cells (Figure 2D). Coculture supernatants were then introduced into a migration assay. To prove that migration towards coculture supernatants is CXCL12–CXCR4-specific, Nalm6 cells were also pretreated with the CXCR4 antagonist AMD3100. Supernatants of both BM-MSC- and testis-derived stromal cell cultures induced strong Nalm6 cell migration, which was significantly inhibited by pretreatment with AMD3100 (Figure 2E). We conclude that CXCL12 is secreted by BM-MSC or testis-derived stromal cells and facilitates migration of CXCR4-expressing Nalm6 cells. Next,

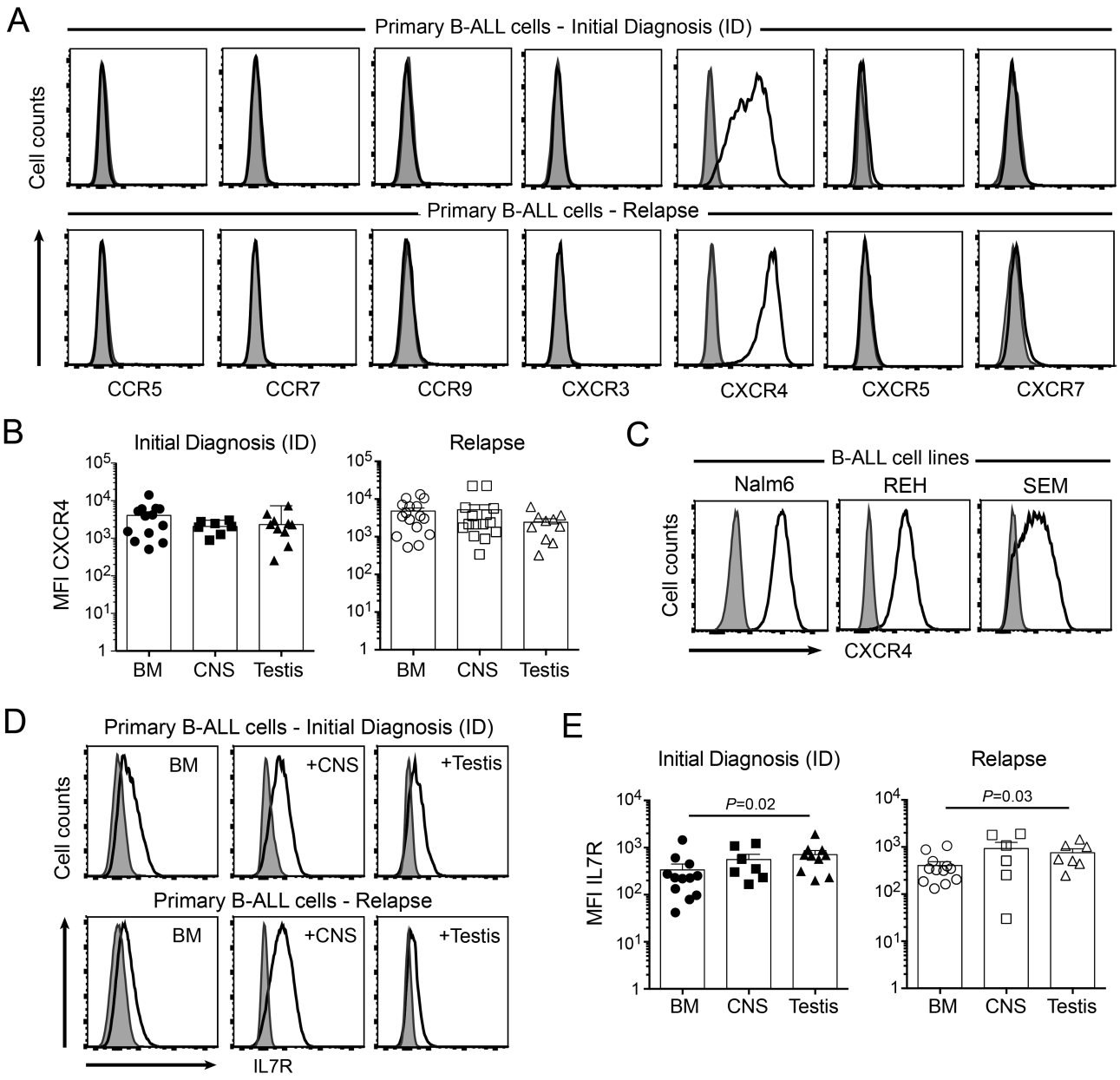

Figure 1. CXCR4 is strongly expressed on primary B-ALL cells at the initial diagnosis as well as during relapse. (A) Primary B-ALL patient samples from bone marrow (BM) at initial diagnosis ($n = 30$) and during relapse ($n = 25$) analyzed for surface expression of various chemokine receptors. Representative histograms show high CXCR4 expression (black line) compared to isotype controls (filled curve) on BM-derived B-ALL samples from patients at initial diagnosis (ID) and at relapse diagnosis with testicular involvement. (B) CXCR4 expression on bone marrow (BM)-derived B-ALL samples taken at ID and at isolated BM ($n = 13$–16), or combined CNS ($n = 7$–13), or testis relapse ($n = 10$) quantitated as mean fluorescence intensity (MFI) normalized against an isotype control. (C) Representative histograms show high CXCR4 expression on three different B-ALL cell lines (REH, Nalm6, SEM; CXCR4, black line; isotype control, filled curve). IL7R expression depicted in (D) representative histograms (black line) compared to isotype control (filled curve) on B-ALL samples at ID and at isolated BM ($n = 12$ in each group), or combined CNS (ID: $n = 7$, relapse: $n = 6$), or combined testis relapse (ID: $n = 10$, relapse: $n = 7$) and (E) quantitated as MFI normalized to isotype control. Data are displayed as single cells and bars represent mean ± SEM, *P* values were calculated using the Mann–Whitney *U* test.

13 primary ALL samples were cocultured for 48 or 72 h without or with 11 BM-MSC and nine testis stroma cell preparations and then analyzed for the proportion of viable (Annexin$^-$7AAD$^-$), and apoptotic (Annexin$^+$) tumor cells (Figure 2F). Both BM- and testis-derived stroma reduced the apoptotic fraction and increased the viable ALL proportion in the tumor-stroma cocultures compared to tumor cells alone. Taken together, these data show that testicular stroma and BM-MSCs can secrete CXCL12 and support survival of primary ALL cells in cocultures.

Sertoli cells and peritubular myoid cells represent part of seminiferous tubules and support ALL cell survival

Sertoli cells and peritubular myoid cells (PTCs) constitute the microenvironmental niche of testis, which is

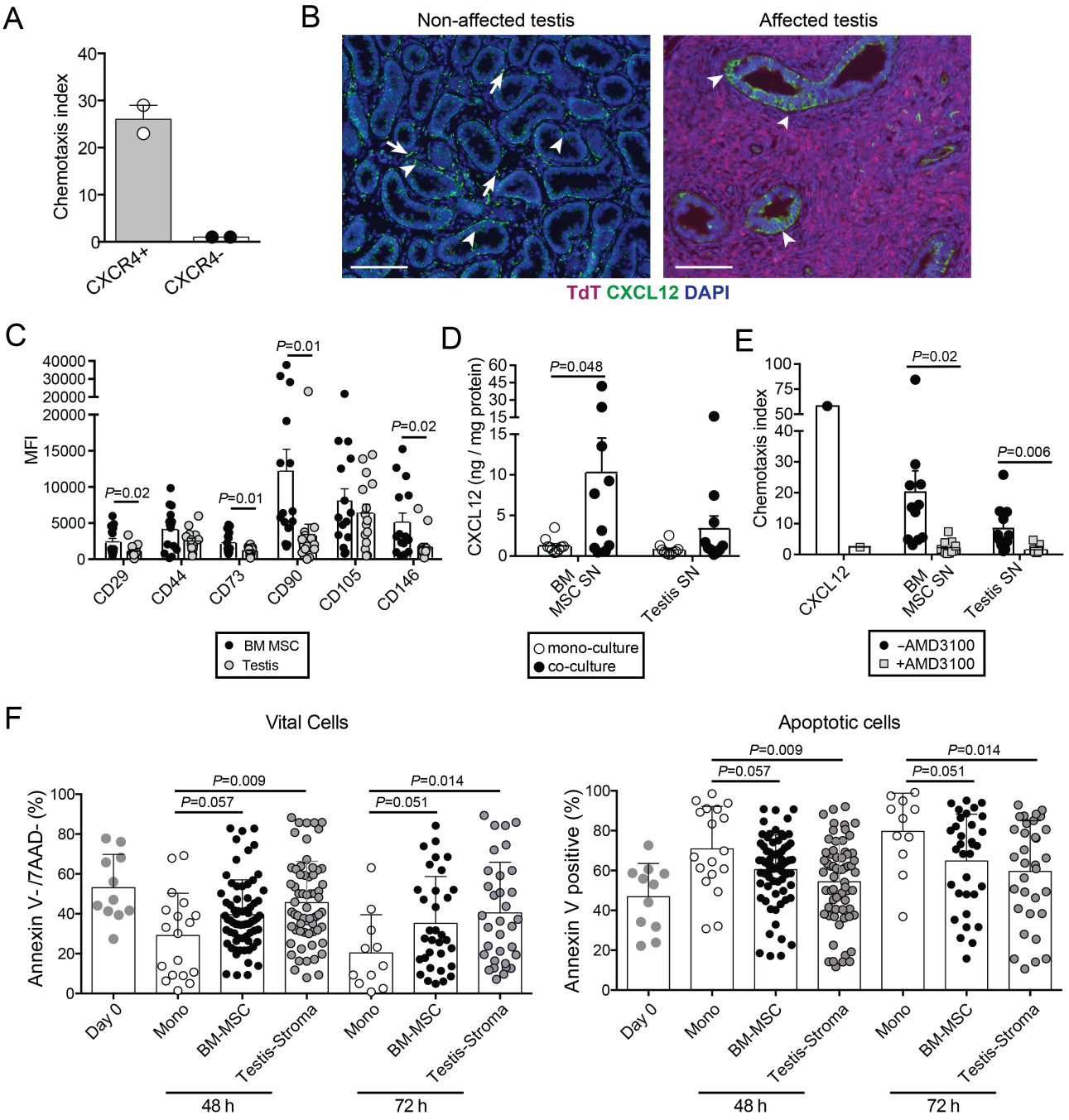

Figure 2. BM- and testis-derived stroma cells support ALL cell survival and secrete CXCL12 that mediates chemotaxis of CXCR4-expressing tumor cells. (A) Inhibition of CXCR4-mediated migration towards human CXCL12 by genetic knockout of *CXCR4* in Nalm6 cells ($n = 2$). (B) Microscopic analysis of CXCL12 expression (green) and TdT-expressing ALL cells (red) in sections of affected and nonaffected testis counterstained with DAPI (blue). Representative sections of $n = 3$ analyzed testes are shown. White arrowheads depict CXCL12 expression by Sertoli cells; white arrows depict CXCL12 expression by unknown stroma cells. Scale bar, 100 µm. (C) Expression of characteristic MSC surface markers (as indicated in the figure) on cultured BM-MSC or testicular stroma cells. Expression was quantitated as mean fluorescence intensity (MFI) normalized against a fluorescence minus one (FMO) ($n = 14$–15). (D) The supernatants of mono- or cocultured stroma cells analyzed for CXCL12 secretion after 72 h by MSD U-Plex technology. CXCL12 levels were normalized to total protein measured by the Bradford assay (BM-MSC $n = 10$, Testis $n = 10$). (E) Nalm6 cell migration towards medium supplemented with 100 nM CXCL12, and towards supernatant of cultured BM-MSC or testicular stroma cells, pretreated without or with the CXCR4 inhibitor AMD3100 analyzed in a Transwell chemotaxis assay (BM-MSC $n = 11$, Testis $n = 11$). (F) The frequency of viable (Annexin$^-$7-AAD$^-$), and apoptotic (Annexin$^+$) primary patient ALL cells ($n = 13$) cocultured without (monoculture; mono), with BM-MSCs, or with testicular stroma cells for 48 or 72 h determined with Annexin/7-AAD staining. Single data points are shown; bars present mean ± SEM; (day 0 $n = 11$, mono 48 h $n = 18$, BM-MSC 48 h $n = 68$, testis 48 h $n = 64$, mono 72 h $n = 11$, BM-MSC 72 h $n = 33$, testis 72 h $n = 33$; primary ALL samples were employed several times, but on different MSCs). *P* values were calculated using a Mann–Whitney *U* test. BM-MSC, bone marrow mesenchymal stem cells.

essential for regulating normal spermatogenesis [27–29]. Because the availability of fresh benign testicular tissue is limited and isolation of stroma cell subpopulations therefore challenging, we isolated Sertoli and PTC cells from mouse testis (supplementary material Figure S3A). Sertoli and PTC cells were seeded,

and purity (>95%) was established by immunofluorescence staining for vimentin as a marker for Sertoli cells and alpha-smooth muscle actin (SMA) as a marker for PTCs 4 days postisolation (supplementary material, Figure S3B).

Next, we measured expression of CXCL12 and IL7 by the primary mouse Sertoli cells and PTCs, the BM stroma cell line M210B4, and the Sertoli cell line TM4. The mouse leukemia cell line EL4 served as a negative control. Strong expression of the mRNA was detected in BM and testicular cell lines, in total testis, in testis-isolated PTCs, and moderately in primary Sertoli cells. Interleukin (IL)7 expression was detectable in total testis and testicular primary PTCs and Sertoli cells, but negative or modestly expressed in the cell lines, TM4 and M210B4, respectively (Figure 3A). Immunofluorescence characterized TM4 and primary Sertoli cells by costaining for CXCL12 and SOX9, a transcription factor that differentiates Sertoli from germ line cells [30] (Figure 3B, C). CXCL12 protein expression in testicular sections was detected by immunostaining (supplementary material, Figure S3C). Also, human IL7 protein expression was confirmed in the seminiferous tubules of ALL relapse patient testis sections by immunofluorescence staining (supplementary material, Figure S3D). Overall, the testicular microenvironment provides the necessary factors to mediate leukemia cell recruitment and survival via the CXCL12–CXCR4 and IL7–IL7R signaling axes.

To support this notion, we prepared cocultures of pediatric patient-derived ALL xenografts (PDX-ALLs) with stromal cell lines or primary testicular stromal cells. The PDX-ALL samples, #1064 and #1476, expressed CXCR4 but no other chemokine receptors (supplementary material, Table S4, and Figure 3D). IL7R was strongly expressed on the PDX-ALL #1064 but not on the #1476 sample (Figure 3D). In a migration assay, #1064 cells showed superior migratory capacity (Figure 3E), possibly due to their higher CXCR4 expression compared to #1476 cells (Figure 3D). Cocultures of #1064 cells with stromal cells revealed enhanced viability when cultured with the BM stromal cell line M210B4 and with primary testicular PTCs, which was further increased by adding IL7 to the cocultures. This effect could not be seen for the PDX-ALL sample #1476, which only exhibited minor IL7R expression. Here, only the coculture with primary NSG PTCs led to an increased survival but this effect was independent of IL7 (Figure 3F).

Development of an *in vivo* PDX-ALL mouse model with testicular involvement

Mouse models of acute leukemia with testicular involvement are rare and previous models have not investigated the mechanism of testicular tumor cell dissemination [31–33]. We established a PDX-ALL mouse model with testicular involvement. For noninvasive bioluminescence imaging, PDX-ALL samples were transduced with a luciferase-GFP (Luc^+) construct. Two rounds of transfer in NSG mice and subsequent FACS-sorting yielded Luc^+ leukemic cells with a purity of >98% (supplementary material, Figure S4A,B). Six to 7 weeks after i.v. transfer of 1×10^6 Luc^+ PDX-ALL cells, expansion and BM dissemination of the PDX-ALL cell samples could be monitored by IVIS imaging (supplementary material, Figure S4C).

Because testicular infiltration is mainly observed in pediatric patients, we hypothesized that testicular infiltration might be dependent on a prepuberty state. We transferred 1×10^6 or 1×10^4 PDX-ALL cells i.v. in 8–12 (postpuberty) or in 3–3.5 (prepuberty) week-old mice and monitored leukemia development by IVIS imaging over 5–8 weeks (Figure 4A). Mice that received 1×10^6 leukemic cells progressed faster than mice that received 1×10^4 leukemic cells. Subsequently, they had to be killed within 35-days, whereas mice that received fewer cells were sacrificed at day 49–52 after transfer (Figure 4A–C depicts mice that received 1×10^4 cells). The frequency of leukemic cells among all hematopoietic cells was determined in testis, BM, and spleen (Figure 4D). Testicular dissemination was highest when a low number of #1064 leukemic cells were transferred in prepuberty mice, whereas dissemination in BM and spleen was equally high regardless of the cell numbers or the recipients age. Notably, the PDX-ALL sample #1476, which exhibited reduced *in vitro* migratory capability towards CXCL12 and weak IL7R expression, showed only minor testicular dissemination (Figure 4E).

Leukemic cells are localized within the interstitial space of mouse and human testis in close contact with interstitial testicular macrophages

Testicular tissue infiltration and distribution of leukemic cells was determined by immunohistochemistry on serial testis sections. As shown exemplarily in Figure 5A, leukemic cells localized in the interstitial space of the mouse testis, comparable to the localization pattern shown for human testicular involvement (Figures 2B and 5C). In human testis sections, we observed leukemic cells in close proximity to $CD206^+CD64^+$ macrophages (Figure 5C,D) The infiltrated areas were assessed in serial sections of testes from pre- and postpuberty mice transplanted with 1×10^4 cells (Figure 5B). This analysis confirmed the observation from the flow cytometry analysis (Figure 4D) that only prepuberty mice show a significant testicular involvement.

Next, we determined the impact of leukemic cell-stroma crosstalk on the polarization of testicular macrophages (TMs) and found that genes associated with an M2 signature, *Marco* and *Arg1*, were significantly upregulated, whereas genes characteristic for M1 macrophages, such as *Cxcl10*, were downregulated in TMs isolated from PDX-ALL-challenged mice

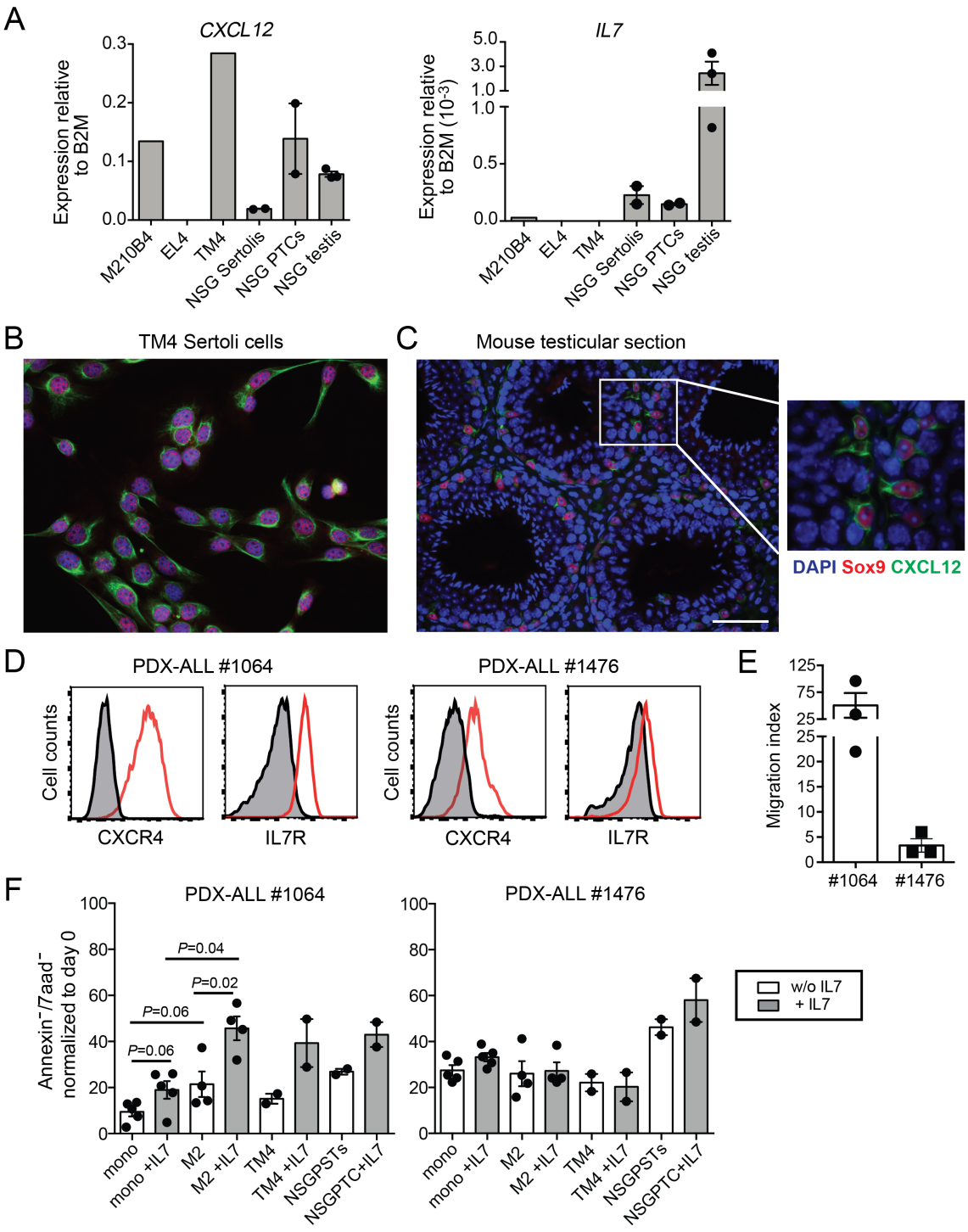

Figure 3. Primary Sertoli cells and murine stroma cell lines express CXCL12 and IL7 and support viability of PDX-ALL cells. (A) Primary mouse Sertoli and PTC cells were generated from NSG mice as described in supplementary material, Figure S3. After culturing Sertoli cells ($n = 2$ independent experiments with cells from testis of 6–10 mice) for four and PTCs ($n = 2$ independent experiments with cells from testis of 6–10 mice) for 7 days, RNA was isolated and expression of *CXCL12* and *IL7* was determined; RNA from the BM cell line M210B4 (M2, $n = 1$), the Sertoli cell line TM4 ($n = 1$), or from whole testis RNA ($n = 3$ mice) served as positive controls; the leukemia cell line EL4 ($n = 1$) as a negative control. Representative images of immunofluorescence showing CXCL12 (green) expression of (B) the Sox9+ Sertoli cell line TM4 (red) and of (C) Sox9+ Sertoli cells (red) in NSG mouse testis sections ($n = 2$). DAPI (blue) was used for nuclear counterstaining. Scale bar, 100 µm. (D) Representative histograms show surface expression of the chemokine receptor CXCR4 and the IL7 receptor IL7R on two luciferized PDX-ALL cell samples (#1064, #1476). Black lined and filled curves represent MFIs of the isotype control and the red line MFIs of the analyzed receptor or adhesion molecule. (E) Migration of CXCR4-expressing PDX-ALL cells towards murine CXCL12 was analyzed in a Transwell chemotaxis assay ($n = 2$ for each PDX-ALL sample). (F) The viability (annexin$^-$/7AAD$^-$) of PDX-ALL samples #1064 and #1476 cocultured without (mono, $n = 5$), with the BM cell line M210B4 ($n = 4$), the Sertoli cell line TM4 ($n = 2$), and primary murine testicular PTCs ($n = 2$) with or without addition of 10 ng/ml human IL7 was determined after 48 h. All data are displayed as individual points, bars present mean ± SEM.

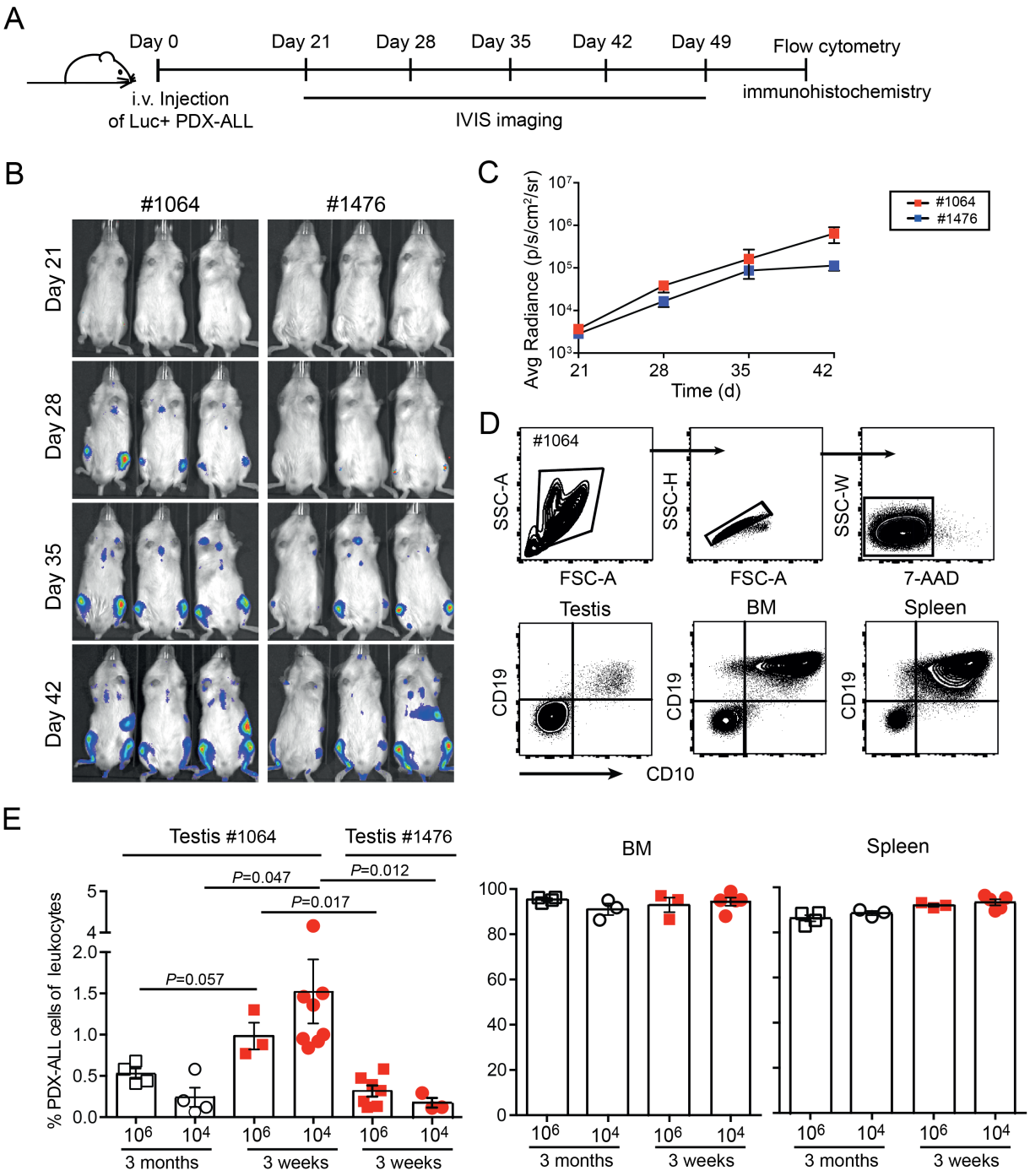

Figure 4. Establishment of a PDX-ALL model with testicular involvement in prepuberty NSG mice. (A) Schematic of the experimental design for the PDX-ALL xenotransplantation model. (B) Engraftment of 1×10^4 i.v. transplanted PDX-ALL was monitored by IVIS imaging and images of serial IVIS-exposures of mice treated with PDX-ALL #1064 or #1476 ($n = 3$ for each group) are shown (exposure time 60 s). (C) Mean ± SEM of the signal intensities obtained from the entire body tumor burden are plotted for each PDX-ALL sample over time. (D) Representative gating (single and 7-AAD$^-$ vital cells) and staining strategy (CD45+ CD19+ CD10+) to identify the percentage of PDX-ALL cells (#1064) of all hematopoietic cells in BM, spleen. and testis. (E) Percentage of recovered PDX-ALL cells (#1064 and #1476) of all cells in testis, BM, and spleen of xenotransplanted 3 month- (postpuberty) or 3 week-old (prepuberty) NSG mice with either 1×10^6 ($n = 3$ or 4 for 3-month-old; $n = 3$–7 for 3-week-old) or 1×10^4 ($n = 3$ or 4, 3-month-old; $n = 3$–8, 3-week-old) PDX-ALL cells. Data are displayed as single cells and bars present mean ± SEM, *P* values were calculated using a Mann–Whitney *U* test.

compared to untreated controls (supplementary material, Figure S5A and Figure 5E). PDX-ALL cells, on the other hand, expressed the TAM-inducing cytokine mRNAs *IL10* and *MCSF* (supplementary material, Figure S5B).

In conclusion, a PDX-ALL mouse model with testicular involvement was established that required the adoptive transfer of PDX-ALL cells in prepuberty mice to allow a detectable testicular dissemination and interstitial localization of leukemic cells.

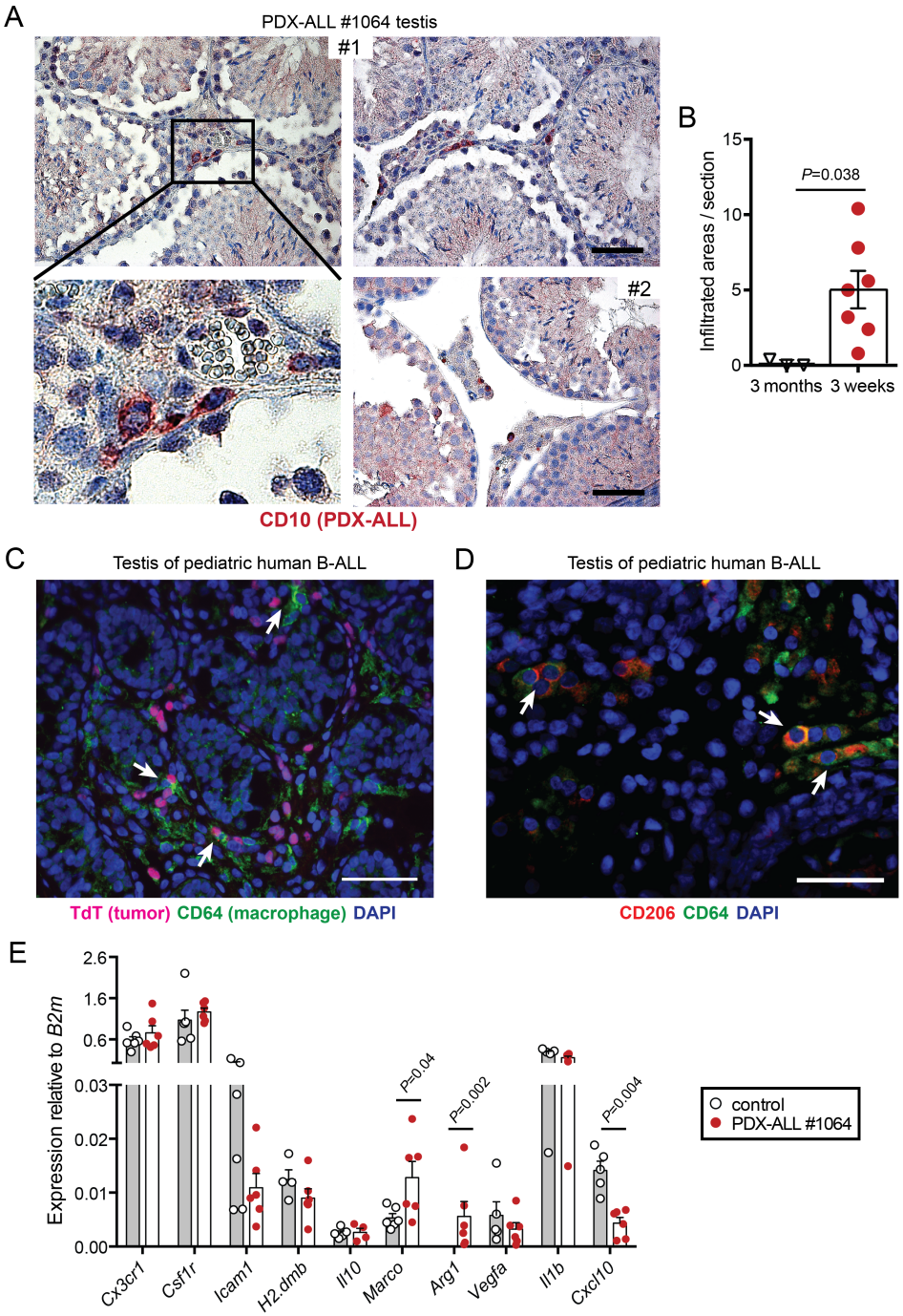

Figure 5. Leukemic cells colocalize with macrophages within the interstitial space of mouse and human testis. (A) Representative immunostaining for CD10$^+$ PDX-ALL cells (in red) in serial testicular sections of mice (#1 and #2 out of $n = 7$ mice are shown, for #1 two testicular sections and one enlarged image are shown) that received 1×10^4 PDX-ALL cells with 3 weeks of age and were analyzed 49 days after xenotransplantation. Scale bars, 50 µm. (B) Infiltrated areas were assessed for PDX-ALL cell infiltration in five sections per mice ($n = 3$ mice for 3-month-old and $n = 7$ for 3-week-old mice). (C,D) Microscopic analysis of (C) TdT-expressing ALL cells (red) in close proximity to CD64$^+$ testicular macrophages (green) and (D) double-stained CD206$^+$CD64$^+$ (orange)-stained macrophages in sections of B-ALL testis counterstained with the nuclear dye DAPI (blue). Representative sections of $n = 3$ analyzed testes are shown. White arrows depict colocalization of leukemic cells with macrophages and CD206$^+$CD64$^+$ double-positive macrophages, respectively. Scale bars, 100 µm. (E) Expression of M1 or M2 surface markers on testicular macrophages isolated from untreated mice (control, $n = 6$) or mice challenged with PDX-ALL cells ($n = 6$). Data are displayed as single cells, bars present mean ± SEM, *P* values were calculated using a Mann–Whitney *U* test.

Testicular leukemic cell engraftment could be inhibited by blocking the CXCL12–CXCR4 signaling axis

CXCR4 is the only homing receptor uniformly and functionally expressed on primary pediatric B-ALLs (Figure 1), and on PDX-ALL samples (Figure 3D). Additionally, CXCL12 expression in testis derived from ALL patients and mice was demonstrated (Figures 2B and 3C). Hence, we envisaged that the CXCL12–CXCR4 signaling axis is crucial for the testicular dissemination of leukemic cells and by that represents a

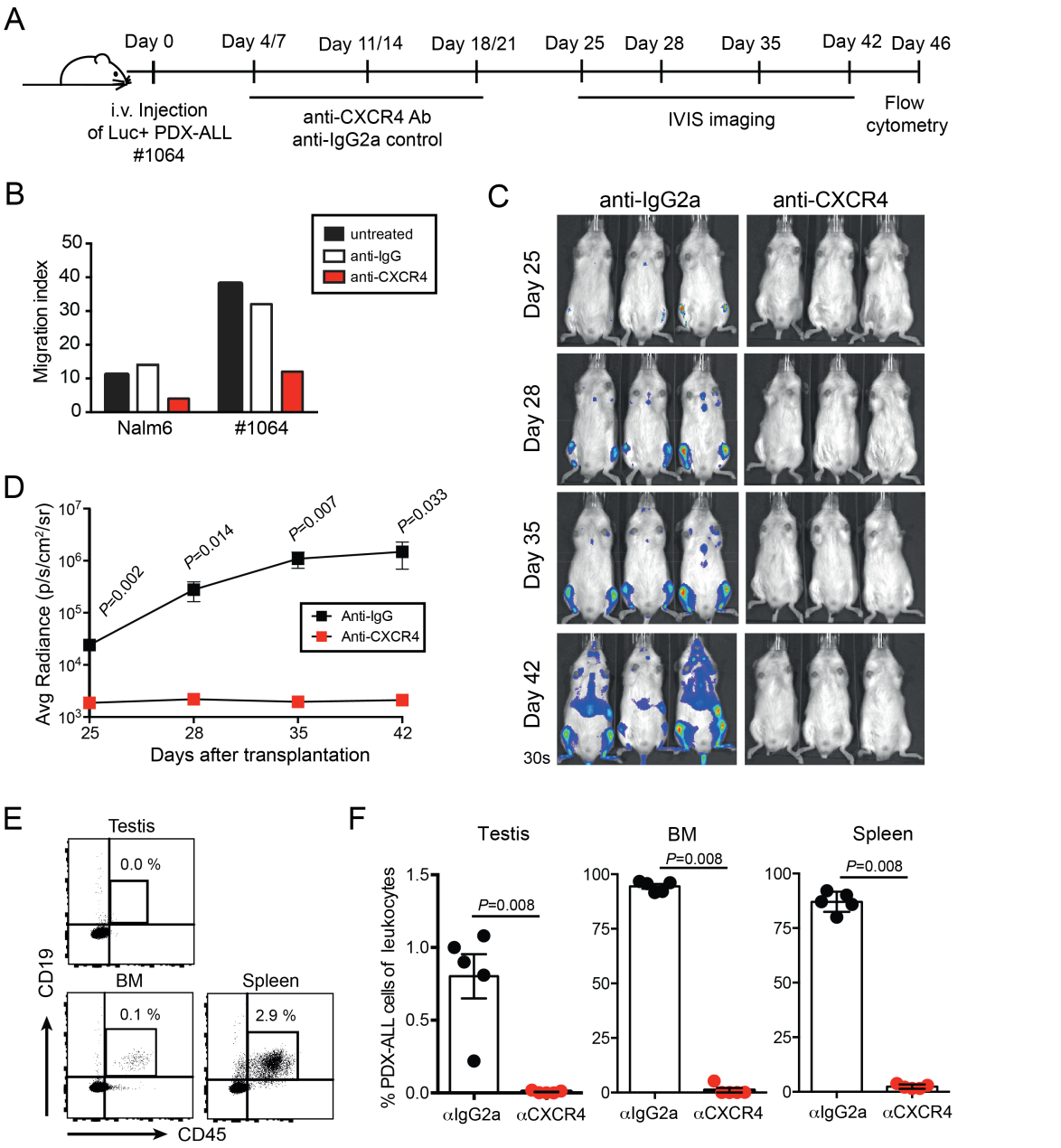

Figure 6. Treatment with an anti-CXCR4 antibody inhibits testicular infiltration of PDX-ALL cells. (A) Schematic of the experimental design for the i.p. anti-CXCR4 treatment in the PDX-ALL xenotransplantation model. (B) Nalm6 or PDX-ALL cells, untreated (black bars), pretreated with an anti-IgG isotype control (open bars) or with the anti-CXCR4 antibody (red bars), for 1 h, were tested in a Transwell chemotaxis assay for their migratory capacity towards CXCL12. (C) The expansion of transplanted cells was monitored by IVIS imaging in anti-CXCR4-treated compared to anti-IgG isotype-treated mice ($n = 3$ per group) over time starting from day 25 up to day 42 (exposure time 30 s). (D) Mean ± SEM of the signal intensities obtained from the entire body tumor burden are plotted for each group over time; *P* values were calculated using an unpaired two-tailed multiple *t* test. At day 49 after transplantation, the percentages of $CD19^{+}CD45^{+}$ PDX-ALL cells of all leukocytes in testis, BM, and spleen were determined in both groups, (E) displays representative dot plots of the anti-CXCR4-treated group and (F) shows the percentages of these cells in anti-CXCR4-treated in comparison to anti-IgG isotype-treated mice with $n = 5$ mice per group from two independent experiments. Data are displayed as single cells; bars present mean ± SEM, *P* values were calculated using a Mann–Whitney *U* test.

potential therapeutic target. Because the CXCL12–CXCR4 signaling axis is also facilitating dissemination of leukemic cells to the BM, we transferred 1×10^4 PDX-ALL #1064 cells in prepuberty mice and started systemic anti-CXCR4 treatment 4 days later to enable initial leukemic cell engraftment to the BM. In two independent experiments, NSG mice were treated from day 4 to day 21 with an anti-CXCR4 or an anti-IgG (isotype control) Ab (Figure 6A and supplementary material, Figure S6A). The inhibitory capability of the anti-CXCR4 Ab was demonstrated by specific block of Nalm6 and PDX-ALL cell migration towards CXCL12 (Figure 6B). Leukemic cell expansion was monitored by IVIS imaging (Figure 6C,D and supplementary material, Figure S6B) and the tumor load was measured on day 46 or day 68 in testis, BM, and spleen (Figure 6A,

E,F). Mice treated with the isotype control showed increasing signals by IVIS imaging, whereas those treated with anti-CXCR4 exhibited no detectable signal during the whole observation time. Small numbers of leukemic cells were found in the BM and spleen of anti-CXCR4-treated mice in contrast to the testes, where no leukemic cells were detectable (Figure 6E,F). In the isotype control group, leukemic cells were detectable in all three organs and the frequencies were comparable to those described in Figure 4E. Notably, total BM-derived hematopoietic cell numbers were unchanged, whereas total splenic cell counts were strongly decreased upon anti-CXCR4 treatment (supplementary material, Figure S6C). Also, CXCR4 expression levels on the remaining tumor cells of BM and spleen were unaltered (supplementary material, Figure S6D). To test if anti-CXCR4 treatment could also prevent or reduce engraftment in testes at a timepoint when leukemia has already progressed, we started treatment 17 days after xenotransplantation when a profound signal in the BM was detectable by IVIS imaging (supplementary material, Figure S7A–C). Anti-CXCR4 Ab treatment was able to abrogate tumor expansion, including dissemination into testes in two out of five mice also at this later timepoint (supplementary material, Figure S7D). However, if the tumor load was too high before starting the treatment, leukemia could no longer be controlled by CXCR4 blockade alone (supplementary material, Figure S7D).

In conclusion, interfering specifically with the CXCL12–CXCR4 signaling axis can prevent testicular dissemination of PDX-ALL cells in a mouse model of B-ALL.

Discussion

Systemic spreading of leukemic cells throughout the organism is tightly regulated by the chemokine/chemokine receptor system. Microenvironmental factors foster the crosstalk between ALL cells and tissue-resident cells, enabling their dissemination and survival at extramedullary sites [22,34].

However, little is known about the mechanisms that causes testis relapse in pediatric B-ALL. We propose that the testis is a frequent site of extramedullary relapse because of the physiologically strong CXCL12 gradient, which is crucial for testis development and spermatogenesis [35,10,11]. We hypothesize that circulating leukemic cells colonize the testes before puberty, and the special immunosuppressive testicular microenvironment at this developmental stage may foster longer periods of dormancy and survival.

We compared the expression of numerous chemokine receptors in a cohort of BM-derived ALL patient samples from initial diagnosis and from different relapse sites: isolated BM relapse, combined BM/CNS relapse, and combined BM/testis relapse. We found that CXCR4 was the only chemokine receptor that was abundantly expressed at the initial diagnosis, as well as at relapse, irrespective of the relapsed site. A synergistic effect between CXCR4 and another surface receptor, IL7R, was reported to regulate not only migration but also malignant transformation [36]. CXCR4 and IL7R interact on the cell surface to recruit BCR-ABL1 and JAK kinases in close proximity, thereby inducing transformation and development of Philadelphia chromosome-positive ALL [36]. Here, we detected increased IL7R expression on B-ALL samples from patients with a combined BM/testis relapse compared to BM relapse only, which points toward a potential link of IL7R expression and testis infiltration. High-level IL7R expression has already been associated with CNS involvement at initial diagnosis and was suggested as a predictor for CNS relapse in pediatric B-ALL [24]. Also, IL7R supported leukemic engraftment and its target inhibition impaired CNS leukemic infiltration in an *in vivo* xenograft model [24]. Taken together, the CXCL12/CXCR4 and the IL7/IL7R axes may jointly facilitate leukemic cell migration and survival to and within the testis niche in pediatric B-ALL.

Testicular relapses occur frequently in boys but not in adult patients, which raises the question whether testicular infiltration by leukemic cells is favored by the prepubertal testicular microenvironment. Testicular macrophages (TMs) support the testis immune-privileged state under developmental and homeostatic conditions. In mice, TMs are subdivided predominantly into MHC^{lo} interstitial (i)TMs and MHC^{hi} peritubular (p)TMs. Specifically, iTMs express immunosuppressive genes and represent the predominant subpopulation in prepuberty mice [37–39]. A suppressed inflammatory environment favors leukemic cell survival and might be further corrupted by leukemic cell interactions with the surrounding testis microenvironment.

A microenvironmental suppressor of an antitumor immune responses are tumor-associated macrophages, TAMs, that can polarize towards a tumor-favorable M2 phenotype not only in solid tumors, but also in B-ALL [40,41]. In line with this, PDX-ALL cells in this study expressed the TAM-inducing cytokines *MCSF* and *IL10*. Overall, this strongly suggests that the testis microenvironment during prepuberty is particularly leukemia-permissive and supportive.

Next, we compared CXCL12 provision by BM- and testis-derived stroma cells. CXCL12 is a crucial chemokine within the BM stem cell niche and produced by BM-MSCs [42,43]. In human testis, CXCL12 is predominantly expressed by Sertoli cells, and it facilitates spermatogonial stem cell migration during spermatogenesis [44]. Here, tumor cell-affected and nonaffected patient testis tissues revealed CXCL12 protein expression in Sertoli cells and other yet undefined interstitial cells. In mouse testis sections, we confirmed strong CXCL12 expression by Sertoli cells. In isolated stromal cell subpopulations, CXCL12 expression was detected by Sertoli cells and PTCs. In line with this, we additionally detected CXCL12 expression in undefined tumor stromal cells from human testis with substantial leukemia involvement. Recent publications have suggested

that under pathological conditions CXCL12 expression is not restricted to Sertoli cells, i.e. CXCL12 is expressed by tumor stroma of seminoma samples [14,45]. *In vitro*, we found enhanced CXCL12 secretion in the supernatant of BM-MSC and testis stroma cultures upon coculture with the B-ALL cell line Nalm6. Both supernatants conferred chemotactic activity to leukemic cells, which was blocked by the specific CXCR4 inhibitor AMD3100 [35]. Moreover, primary B-ALL samples profited from coculturing them with BM-MSC or testis-derived stroma demonstrated by a significant decrease in apoptotic cells compared to the monoculture. Our data show that different testicular cells can provide CXCL12 and that the CXCL12–CXCR4 signaling axis is crucial for recruitment of leukemic cells to the testicular niche. Cells in the interstitial space that potentially provide CXCL12 are Leydig cells and endothelial cells, as shown by Green *et al* [46].

To address the mechanism of testicular involvement *in vivo*, we developed a PDX B-ALL mouse model. To date, only a few B-ALL mouse models with testicular infiltration have been reported. The majority fails to recover a reliable number of testicular leukemic cells and none of them succeeded to demonstrate leukemic cells *in situ* [31–33]. We observed significant testicular infiltration only when xenografts were transferred into prepuberty mice, which strongly indicates that the testicular environment before puberty enables infiltration and survival of leukemic cells. Also, transplanting only 1×10^4 cells instead of 1×10^6 cells led to an increased testicular infiltration, possibly due to the slower tumor progression that allows the cells that initially seeded into the testis to proliferate. Leukemic cell expansion in BM and spleen was indistinguishable in prepuberty and postpuberty recipients, regardless of the numbers of cells that were transplanted. The prepuberty condition was not the only prerequisite for testicular infiltration; the surface expression levels of CXCR4, and potentially of IL7R, on PDX ALL cells were similarly required. When we compared testicular infiltration of xenografts with high CXCR4 and IL7R surface levels (#1064) to xenografts with median CXCR4 and low IL7R levels (#1476), only cells with high CXCR4 and IL7R expression significantly infiltrated testis. An impact of the CXCL12/CXCR4 signaling axis on testicular engraftment has also been suggested by Arnaud *et al* [33]. The tetraspanin CD9, which is overexpressed in *ETV6–RUNX1* fusion gene-positive pediatric B-ALL [47], was shown to support testicular leukemic cell homing through the CXCL12–CXCR4 signaling axis. However, recovered testicular leukemic cell numbers were low and represented only 0.04% of all testis cells. In contrast, our PDX-ALL model showed a robust testicular infiltration of PDX-ALL cells between 1–4% recovered tumor cells. Most important, we demonstrated *in situ* localization of disseminated leukemic cells in the interstitial testicular space, comparable to the localization pattern described for B-ALL patients with testis relapse.

Testicular involvement only occurs in about 30% of the patients, although the CXCL12–CXCR4 signaling axis is physiologically present in testis and ALL blasts widely express CXCR4 regardless of the site of relapse. Most likely, other factors also, such as the expression of the cofactor CD9 and an adapted protumorigenic TME, supports the infiltration and survival of and in the testis.

In line with this suggestion, we have been able to show a functional impact of infiltrated leukemic cells on the polarization of TMs. Five weeks after transfer of PDX-ALL cells, genes associated with an M2 signature, i.e. *Marco* and *Arg11* [48], were upregulated, whereas *Cxcl10*, a gene characteristic for M1 macrophages, was downregulated in TMs of PDX-ALL- challenged mice. This is in line with our published data in which we characterized skewed differentiation of splenic myeloid immune cells in a mouse model of indolent CLL [49].

The importance of the CXCL12–CXCR4 axis for the pathogenesis of leukemia and BM homing has been studied extensively. Disruption of this signaling axis mobilized leukemia cells from their protective BM microenvironment and enhanced susceptibility towards chemotherapy [35]. In pediatric B-cell Precursor (BCP)-ALL patients high CXCR4 protein expression was correlated with an increased risk for relapse and poor overall survival [43]. Numerous CXCR4 antagonists have been developed and tested in combination with chemotherapy or molecular-targeted drugs in clinical trials for acute leukemias, especially in AML and MM [35,50–52].

To investigate whether inhibition of CXCR4 signaling can also interfere with testicular engraftment of PDX-ALL cells in our model, we transferred the CXCR4 high-expressing xenograft #1064 into NSG mice followed by anti-CXCR4 treatment. CXCR4 antibody treatment strongly reduced leukemic infiltration in BM and spleen, and completely abrogated dissemination into the testis. However, when CXCR4 antibody treatment was applied to mice with advanced leukemia, tumor progression was only abrogated in two out of five animals, dependent on the degree of tumor load before treatment.

The present xenotransplantation PDX-ALL model allowed us to apply a systemic blockade of the CXCL12–CXCR4 signaling axis. A limitation of this study is that after an initial seeding of tumor cells, we could not separately block the CXCR4-dependent homing and/or survival of ALL cells to and within BM and testis. Thus, testicular leukemic cell dissemination cannot be separated from the overall progression of leukemia in the BM. Considering this limitation, future dissection of the CXCL12–CXCR4 signaling for testicular relapses will profit from a genetically engineered mouse model in which the CXCL12–CXCR4 axis can be induced and regulated selectively in the testicular tissue.

In summary, we provide some mechanistic insight into how the CXCL12–CXCR4 signaling axis promotes B-ALL cell dissemination and survival under prepubertal microenvironmental conditions at the testis relapse site.

Acknowledgements

The authors thank Armin Rehm for helpful discussions and critical reading of the article. We thank Anthea Wirges and Maria Zschummel for help with the IVIS imaging and the Flow Cytometry platform of the MDC for their technical support.

This work was funded by grants from the Berlin Institute of Health (BIH; K24202000005) to UEH and CE, the HGF 'Zukunftsthema Inflammation & Immunology' (2410085) to UEH, and the German Israeli Foundation (1-1323-422.13/2015) to CE and SI.

Author contributions statement

TS was responsible for methodology, conducting experiments, validating assays, analyzing data, and writing sections of the article. JJJ, MP and KK were responsible for conducting experiments and analyzing data. JPB was responsible for providing resources and technical advice. SI participated in the analysis of data and critical discussion and interpretation of the results. UEH and CE were responsible for all aspects of the study, including the conception and design of the experimental approach, planning, and coordinating experimental procedures, analyzing data, and composing and writing the article. All authors participated in editing and approval of the final text of the article.

References

1. Miranda-Filho A, Piñeros M, Ferlay J, *et al*. Epidemiological patterns of leukaemia in 184 countries: a population-based study. *Lancet Haematol* 2018; **5:** e14–e24.
2. Pui CH, Yang JJ, Hunger SP, *et al*. Childhood acute lymphoblastic leukemia: progress through collaboration. *J Clin Oncol* 2015; **33:** 2938–2948.
3. Henze G, Stackelberg A. Relapsed acute lymphoblastic leukemia. In *Childhood Leukemias* (3rd edn), Pui C-H (ed). Cambridge University Press: Cambridge, 2012; 367–382.
4. Chen-Santel C, Ulrike T, van Schewick C, *et al*. Bilateral involvement is an independent risk factor in testicular relapse of childhood ALL: results of the trials ALL-REZ BFM 83 - 2002. *Blood* 2014; **124:** 66.
5. Gandemer V, Chevret S, Petit A, *et al*. Excellent prognosis of late relapses of ETV6/RUNX1-positive childhood acute lymphoblastic leukemia: lessons from the FRALLE 93 protocol. *Haematologica* 2012; **97:** 1743–1750.
6. Jayakrishnan T, Shaikh H, Samhouri Y, *et al*. Isolated testicular recurrence of B cell acute lymphoblastic leukaemia in an adult: rare case. *BMJ Case Rep* 2019; **12:** e232286.
7. Locatelli F, Schrappe M, Bernardo ME, *et al*. How I treat relapsed childhood acute lymphoblastic leukemia. *Blood* 2012; **120:** 2807–2816.
8. Tokoyoda K, Egawa T, Sugiyama T, *et al*. Cellular niches controlling B lymphocyte behavior within bone marrow during development. *Immunity* 2004; **20:** 707–718.
9. Burger JA, Bürkle A. The CXCR4 chemokine receptor in acute and chronic leukaemia: a marrow homing receptor and potential therapeutic target. *Br J Haematol* 2007; **137:** 288–296.
10. Méndez-Ferrer S, Bonnet D, Steensma DP, *et al*. Bone marrow niches in haematological malignancies. *Nat Rev Cancer* 2020; **20:** 285–298.
11. Crazzolara R, Kreczy A, Mann G, *et al*. High expression of the chemokine receptor CXCR4 predicts extramedullary organ infiltration in childhood acute lymphoblastic leukaemia. *Br J Haematol* 2001; **115:** 545–553.
12. Guo F, Wang Y, Liu J, *et al*. CXCL12/CXCR4: a symbiotic bridge linking cancer cells and their stromal neighbors in oncogenic communication networks. *Oncogene* 2016; **35:** 816–826.
13. Gilbert DC, Chandler I, McIntyre A, *et al*. Clinical and biological significance of CXCL12 and CXCR4 expression in adult testes and germ cell tumours of adults and adolescents. *J Pathol* 2009; **217:** 94–102.
14. McIver SC, Loveland KL, Roman SD, *et al*. The chemokine CXCL12 and its receptor CXCR4 are implicated in human seminoma metastasis. *Andrology* 2013; **1:** 517–529.
15. Westernströer B, Langenstroth D, Kliesch S, *et al*. Developmental expression patterns of chemokines CXCL11, CXCL12 and their receptor CXCR7 in testes of common marmoset and human. *Cell Tissue Res* 2015; **361:** 885–898.
16. Fijak M, Meinhardt A. The testis in immune privilege. *Immunol Rev* 2006; **213:** 66–81.
17. Winnall WR, Hedger MP. Phenotypic and functional heterogeneity of the testicular macrophage population: a new regulatory model. *J Reprod Immunol* 2013; **97:** 147–158.
18. Lokka E, Lintukorpi L, Cisneros-Montalvo S, *et al*. Generation, localization and functions of macrophages during the development of testis. *Nat Commun* 2020; **11:** 4375.
19. Mossadegh-Keller N, Gentek R, Gimenez G, *et al*. Developmental origin and maintenance of distinct testicular macrophage populations. *J Exp Med* 2017; **214:** 2829–2841.
20. Shalapour S, Eckert C, Seeger K, *et al*. Leukemia-associated genetic aberrations in mesenchymal stem cells of children with acute lymphoblastic leukemia. *J Mol Med (Berl)* 2010; **88:** 249–265.
21. Bluhm J, Kieback E, Marino SF, *et al*. CAR T cells with enhanced sensitivity to B cell maturation antigen for the targeting of B cell non-Hodgkin's lymphoma and multiple myeloma. *Mol Ther* 2018; **26:** 1906–1920.
22. Höpken UE, Rehm A. Homeostatic chemokines guide lymphoma cells to tumor growth-promoting niches within secondary lymphoid organs. *J Mol Med (Berl)* 2012; **90:** 1237–1245.
23. Höpken UE, Rehm A. Targeting the tumor microenvironment of leukemia and lymphoma. *Trends Cancer* 2019; **5:** 351–364.
24. Alsadeq A, Lenk L, Vadakumchery A, *et al*. IL7R is associated with CNS infiltration and relapse in pediatric B-cell precursor acute lymphoblastic leukemia. *Blood* 2018; **132:** 1614–1617.
25. Pal D, Blair HJ, Elder A, *et al*. Long-term in vitro maintenance of clonal abundance and leukaemia-initiating potential in acute lymphoblastic leukaemia. *Leukemia* 2016; **30:** 1691–1700.
26. de Rooij B, Polak R, van den Berk LCJ, *et al*. Acute lymphoblastic leukemia cells create a leukemic niche without affecting the CXCR4/CXCL12 axis. *Haematologica* 2017; **102:** e389–e393.
27. Griswold MD. The central role of Sertoli cells in spermatogenesis. *Semin Cell Dev Biol* 1998; **9:** 411–416.
28. Zirkin BR, Papadopoulos V. Leydig cells: formation, function, and regulation. *Biol Reprod* 2018; **99:** 101–111.
29. Maekawa M, Kamimura K, Nagano T. Peritubular myoid cells in the testis: their structure and function. *Arch Histol Cytol* 1996; **59:** 1–13.
30. Kanai Y, Hiramatsu R, Matoba S, *et al*. From SRY to SOX9: mammalian testis differentiation. *J Biochem* 2005; **138:** 13–19.
31. Velázquez-Avila M, Balandrán JC, Ramírez-Ramírez D, *et al*. High cortactin expression in B-cell acute lymphoblastic leukemia is associated with increased transendothelial migration and bone marrow relapse. *Leukemia* 2019; **33:** 1337–1348.

32. Jackson H, Jackson NC, Bock M, *et al*. Testicular relapse in acute lymphoblastic leukaemia: studies with an experimental mouse model. *Br J Cancer* 1984; **49:** 73–78.
33. Arnaud MP, Vallée A, Robert G, *et al*. CD9, a key actor in the dissemination of lymphoblastic leukemia, modulating CXCR4-mediated migration via RAC1 signaling. *Blood* 2015; **126:** 1802–1812.
34. Pals ST, de Gorter DJ, Spaargaren M. Lymphoma dissemination: the other face of lymphocyte homing. *Blood* 2007; **110:** 3102–3111.
35. Burger JA, Peled A. CXCR4 antagonists: targeting the microenvironment in leukemia and other cancers. *Leukemia* 2009; **23:** 43–52.
36. Abdelrasoul H, Vadakumchery A, Werner M, *et al*. Synergism between IL7R and CXCR4 drives BCR-ABL induced transformation in Philadelphia chromosome-positive acute lymphoblastic leukemia. *Nat Commun* 2020; **11:** 3194.
37. Bhushan S, Tchatalbachev S, Lu Y, *et al*. Differential activation of inflammatory pathways in testicular macrophages provides a rationale for their subdued inflammatory capacity. *J Immunol* 2015; **194:** 5455–5464.
38. Winnall WR, Muir JA, Hedger MP. Rat resident testicular macrophages have an alternatively activated phenotype and constitutively produce interleukin-10 in vitro. *J Leukoc Biol* 2011; **90:** 133–143.
39. Bhushan S, Theas MS, Guazzone VA, *et al*. Immune cell subtypes and their function in the testis. *Front Immunol* 2020; **11:** 583304.
40. Mantovani A, Sozzani S, Locati M, *et al*. Macrophage polarization: tumor-associated macrophages as a paradigm for polarized M2 mononuclear phagocytes. *Trends Immunol* 2002; **23:** 549–555.
41. Chen SY, Yang X, Feng WL, *et al*. Organ-specific microenvironment modifies diverse functional and phenotypic characteristics of leukemia-associated macrophages in mouse T cell acute lymphoblastic leukemia. *J Immunol* 2015; **194:** 2919–2929.
42. Peled A, Petit I, Kollet O, *et al*. Dependence of human stem cell engraftment and repopulation of NOD/SCID mice on CXCR4. *Science* 1999; **283:** 845–848.
43. van den Berk LC, van der Veer A, Willemse ME, *et al*. Disturbed CXCR4/CXCL12 axis in paediatric precursor B-cell acute lymphoblastic leukaemia. *Br J Haematol* 2014; **166:** 240–249.
44. Yang QE, Kim D, Kaucher A, *et al*. CXCL12-CXCR4 signaling is required for the maintenance of mouse spermatogonial stem cells. *J Cell Sci* 2013; **126:** 1009–1020.
45. Gaudichon J, Jakobczyk H, Debaize L, *et al*. Mechanisms of extramedullary relapse in acute lymphoblastic leukemia: reconciling biological concepts and clinical issues. *Blood Rev* 2019; **36:** 40–56.
46. Green CD, Ma Q, Manske GL, *et al*. A comprehensive roadmap of murine spermatogenesis defined by single-cell RNA-Seq. *Dev Cell* 2018; **46:** 651–667.e10.
47. Gandemer V, Aubry M, Roussel M, *et al*. CD9 expression can be used to predict childhood TEL/AML1-positive acute lymphoblastic leukemia: proposal for an accelerated diagnostic flowchart. *Leuk Res* 2010; **34:** 430–437.
48. Orecchioni M, Ghosheh Y, Pramod AB, *et al*. Macrophage polarization: different gene signatures in M1(LPS+) vs. classically and M2(LPS-) vs. alternatively activated macrophages. *Front Immunol* 2019; **10:** 1084.
49. Gätjen M, Brand F, Grau M, *et al*. Splenic marginal zone granulocytes acquire an accentuated neutrophil B-cell helper phenotype in chronic lymphocytic leukemia. *Cancer Res* 2016; **76:** 5253–5265.
50. Cancilla D, Rettig MP, DiPersio JF. Targeting CXCR4 in AML and ALL. *Front Oncol* 2020; **10:** 1672.
51. Zhang Y, Saavedra E, Tang R, *et al*. Targeting primary acute myeloid leukemia with a new CXCR4 antagonist IgG1 antibody (PF-06747143). *Sci Rep* 2017; **7:** 7305.
52. Li L, Chai Y, Wu C, *et al*. Chemokine receptor CXCR4: an important player affecting the molecular-targeted drugs commonly used in hematological malignancies. *Expert Rev Hematol* 2020; **13:** 1387–1396.
53. Pham H, Tonai R, Wu M, *et al*. CD73, CD90, CD105 and Cadherin-11 RT-PCR screening for mesenchymal stem cells from cryopreserved human cord tissue. *Int J Stem Cells* 2018; **11:** 26–38.
54. Harkness L, Zaher W, Ditzel N, *et al*. CD146/MCAM defines functionality of human bone marrow stromal stem cell populations. *Stem Cell Res Ther* 2016; **7:** 4.
55. Kauerhof AC, Nicolas N, Bhushan S, *et al*. Investigation of activin A in inflammatory responses of the testis and its role in the development of testicular fibrosis. *Hum Reprod* 2019; **34:** 1536–1550.
56. Bhushan S, Aslani F, Zhang Z, *et al*. Isolation of Sertoli cells and peritubular cells from rat testes. *J Vis Exp* 2016: (**108**): e53389.

References 53–56 are cited only in the supplementary material.

SUPPLEMENTARY MATERIAL ONLINE

Supplementary materials and methods

Figure S1. Generation of a Nalm6-CXCR4 KO cell line

Figure S2. CXCL12 protein expression in B-ALL affected testis

Figure S3. Staining of isolated and cultured of testicular Sertoli and PTC cells and testis sections

Figure S4. Generation of luciferase-GFP stably expressing PDX-ALL cells by lentiviral transduction

Figure S5. Isolation of testicular macrophages from NSG mice and expression of TAM-inducing cytokines by PDX-ALL cells

Figure S6. Treatment with an anti-CXCR4 antibody inhibits engraftment of PDX-ALL cells

Figure S7. Treatment of advanced leukemia with an anti-CXCR4 antibody partially inhibits progression of PDX-ALL

Table S1. Disease characteristics of primary patient samples used for generation of human B-ALL xenografts

Table S2. Oligonucleotide primers for RT-qPCR using TaqMan probes

Table S3. Chemokine receptor expression of primary B-ALL patient cell samples

Table S4. Chemokine receptor expression of PDX-ALL cell samples